ORIGINAL ARTICLE

New phenomenological model for comparison of lasers with different temporal outputs

Julio Coroado[1] · Stewart Williams[1] · Wojciech Suder[1] · Supriyo Ganguly[1] · Sonia Meco[1] · Goncalo Pardal[1]

Abstract

Laser welding is distinguished by low heat input, low distortion, high travel speeds and accuracy. Traditional high-power pulsed wave (PW) lasers are being replaced by high-frequency low-pulse energy fibre lasers. However, as these lasers operate at very high frequencies, near continuous wave (CW) operation, it is not clear the benefit of such frequencies in comparison to CW lasers for micro-welding. In this project, two lasers, one in high-frequency PW and another in CW are operated at the same conditions, including average power, average peak power, spot size and travel speed, and the differences in material response are investigated. It has been shown that frequency is one of the important parameters that affect the heat loss between individual pulses, referred to as inter-pulse losses. At low frequency, the PW laser provided lower melting efficiency and higher penetration efficiency than CW. On the other hand, at high frequency, the PW resulted in lower melting and penetration efficiency than CW. In addition, a new definition of interaction time has been proposed to capture conduction losses by travel speed and heat inter-pulse losses due to periodic lack of laser power. This allows a like-for-like comparison of CW and PW lasers and can be used to predict penetration depth with processing parameters.

Keywords Laser welding · CW and PW modes · Inter-pulse spacing · Weld shape · Stainless steel

1 Introduction

Product miniaturisation is leading to the development of new techniques for the joining of micro-scale components, with particular attention on electronic products and automobiles [1]. Laser is one of the most commonly used non-contact processes in micro-welding applications to join similar [2] and dissimilar alloys [3, 4]. Its high accuracy and flexibility of spatial and temporal energy resolution allows components to be welded and parts to be 3D printed with low heat input, leading to low thermal distortion and residual stresses in the workpiece, when compared to other processes [5–7].

Fibre delivery of laser energy has several benefits for industrial purposes, such as compact size, flexible beam delivery, high efficiency, and low maintenance costs. The relatively short wavelength (1 μm) and good focus-ability makes fibre lasers a suitable tool for micro-scale welding applications [8]. One of the most important characteristics

of these systems is the temporal mode: pulsed-wave (PW) or continuous-wave (CW). In single-pulse PW (SPPW) welding, the energy is delivered in relatively long pulses (milliseconds) at low frequency, high peak power and high pulse energy, with the processing speed generally slow [9]. However, the old Nd-YAG flash pumped lasers are being replaced by the new generation of multi-pulse PW (MPPW) fibre lasers, which cannot provide such high pulse energy in a single pulse as the flash pumped lasers, but as they are operated at high frequencies (kHz) and shorter pulse durations (nanoseconds), the energy application for processing materials is highly flexible. The main difference between SPPW and MPPW is that in MPPW, the energy accumulates between pulses. This means that the inter-pulse spacing has a major effect on the thermal behaviour and resultant melt profile. The pulse shape plays an important role in controlling the temperature distribution in the processed metal [10]. For low peak power, the heat is transferred to the material by conduction, but if it is increased above a certain threshold [11], a keyhole is formed, enhancing the laser absorptivity in the material and increasing penetration depth. For high peak power and constant pulse energy, spatter and crack propagation

✉ Julio Coroado
  julio.coroado@gmail.com

1 Welding Engineering and Laser Processing Centre, Cranfield University, Cranfield MK43 0AL, UK

can be an issue due to the rapid thermal cycle [12]. The pulse duration is also responsible for the control of the heat input into the metal, with the amount of molten metal being reduced for shorter pulses.

CW lasers are less flexible than PW as the parameter's selection is shorter, but in general, offer higher maximum average powers and can be applied to a wider range of material thicknesses. The high penetration and good melt pool stability and weld quality of CW mode are attributed to the continuous delivery of energy to the metal since the peak power is always constant and relatively low during the irradiation time [13]. However, to minimise the high heat input, which is necessary for micro-welding applications, CW lasers have to be operated at higher processing speeds than PW lasers to avoid the vaporisation of the alloying elements of the base materials, which is not always practically possible [14, 15].

To select the most optimum process for a given application, it is important to consider whether a CW laser with low peak power but operated at high travel speed is more appropriate than a PW laser operated at lower speed and frequency but at higher peak power. Most of the experimental works, reported in the literature, presented results for one type of processing mode only, and there is limited knowledge on understanding which temporal mode has higher penetration and melting efficiency due to the lack of comparable parameters. Assuncao and Williams [16] have studied SPPW and CW welding at the same interaction time and power density and showed that the former had a much higher penetration depth, resulting in a lower heat input required to achieve similar penetration. They attributed this to the difference in surface tension gradient and its effect on fluid flows. Demir et al. have compared MPPW and CW lasers [17]. They found that MPPW welding was more suitable for thin and precise applications due to the high power densities, giving rise to vaporisation and a recoil effect, and resulting in lower average power usage [18], whereas the weld quality achieved with CW laser was superior, with less porosity. Biffi et al. achieved finer microstructures in MPPW welding, while the increased thermal load in CW welding resulted in larger weld pools and better mechanical properties [7]. However, most of the reported studies were made based on different system parameters, such as spot size and travel speed, which resulted in completely different applied energies and power densities, making the effect of temporal mode difficult to unravel.

The fundamental laser-material interaction parameters (FLMIPs) can be used in CW [19, 20] and MPPW [21] laser systems to achieve similar weld shapes through the control of the weld thermal cycle. The weld width is controlled by the laser-material interaction time and the thermal properties of the material. The total energy input drives the heat conduction and convection downwards and laterally, increasing the penetration depth and widening the melt pool. Therefore, the weld width is much larger than the laser spot size, being independent of it [22]. However, similar weld shapes may not be replicated in other temporal modes and different materials even if similar FLMIPs are used. The material's thermal properties and the thermal losses created by different travel speeds, spot sizes, laser duty cycles and frequencies affect the weld pool formation and need to be captured in the formulae of laser-material interaction time and applied energy. This work aims to compare CW and MPPW modes under similar welding conditions using a set of new parameters proposed to capture thermal behaviour due to the laser temporal mode and material properties. A list of abbreviations of the processing parameters used throughout this work is presented in Table 1.

2 Fundamentals of welding regimes and parameters

2.1 CW welding

In CW mode, the fundamental laser-material interaction parameters are the laser-material interaction time ($t_{i, CW}$), average power density (q_p), and specific point energy ($E_{SP, CW}$) [23]. Interaction time defines the time, in which a particular point in the weld centreline is exposed to the laser beam, whilst the beam is moving at a constant speed. This is similar to the pulse duration from the SPPW laser welding and corresponds to discrete unit time [23]. The average power density (q_p) is one of the fundamental parameters that define optical power per unit area and is given by Eq. (1), where P_L is the laser average output power, and A_S is the area of the laser spot on the material's surface.

$$q_p = P_L/A_s (\text{MW/cm}^2) \qquad (1)$$

Laser welding is considered a periodic process, whose period is the interaction time. Therefore, the energy delivered to the laser spot, denoted as the specific point energy, is given by Eq. (2) [23]:

$$E_{SP, CW} = q_p t_{i, cw} A_s (J) \qquad (2)$$

The energy rate transferred into the material depends on the travel speed, which controls global thermal losses to the periphery of the melt pool. A typical thermal cycle of a CW weld is shown in Fig. 1.

Table 1 List of abbreviations

Abbreviation	Description	Units
P_L	Average output power	W
v	Travel speed	mm/s
d	Beam diameter	μm
A_S	Area of the laser beam size on the material surface	mm^2
PRF	Pulse repetition frequency	kHz
PRF_0	Pulse repetition frequency at maximum pulse energy and peak power	kHz
$t_{i,\,CW}$	Interaction time in CW mode	ms
$t_{i,\,SPPW}$	Interaction time in single-pulse PW mode	ms
$t_{i,\,MPPW\,(old)}$	Old interaction time in multi-pulse PW mode	ms
$t_{i,\,MPPW\,(new)}$	New interaction time in multi-pulse PW mode	ms
t_0	Material characteristic thermal time	μs
P_{peak}	Average peak power	kW
E_{pulse}	Pulse energy	mJ
P_{Width}	Pulse width	ns
q_p	Average power density	MW/cm^2
$q_{p,\,peak}$	Average peak power density	MW/cm^2
$E_{SP,\,cw}$	Specific point energy in CW mode	mJ
$E_{SP,\,MPPW\,(old)}$	Old specific point energy in multi-pulse PW mode	mJ
$E_{SP,\,MPPW\,(new)}$	New specific point energy in multi-pulse PW mode	mJ
I_S	Inter-pulse spacing	μs
DC	Duty cycle	%
O_F	Overlap factor	%
M_{Eff}	Melting efficiency	J/mm^3
P_{Eff}	Penetration efficiency	J/mm

2.2 PW welding

2.2.1 Single-pulse

In SPPW welding, the energy is delivered in individual pulses with a characteristic peak power (P_{peak}), pulse energy (E_{pulse}) and pulse duration (P_{Width}). In the conventional millisecond SPPW operation, the pulse shape can be rectangular, with constant peak power which is significantly higher than the average power [24]. The space between pulses is sufficient to allow complete energy dissipation in the material before the next pulse is incident on the surface. The weld thermal cycle is shown schematically in Fig. 2.
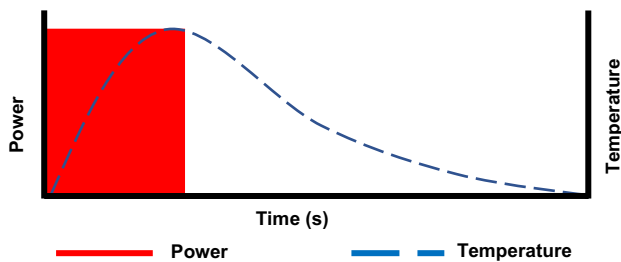
2.2.2 Multi-pulse

MPPW welding is more complex than SPPW due to energy build up and transient thermal cycle between the pulses. As shown in Fig. 3, the pulse shape of a nanosecond MPPW laser can be modulated. The power distribution is not constant and changes with the frequency, being the peak power and pulse energy maximum at a certain frequency (PRF_0) and average power. For frequencies higher than PRF_0, the peak power and pulse energy decrease, becoming the pulse shape almost square. Since the peak power lasts only a few nanoseconds, the average of the power distribution within a pulse can be used to simplify
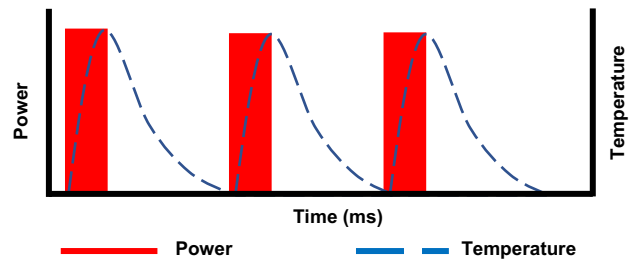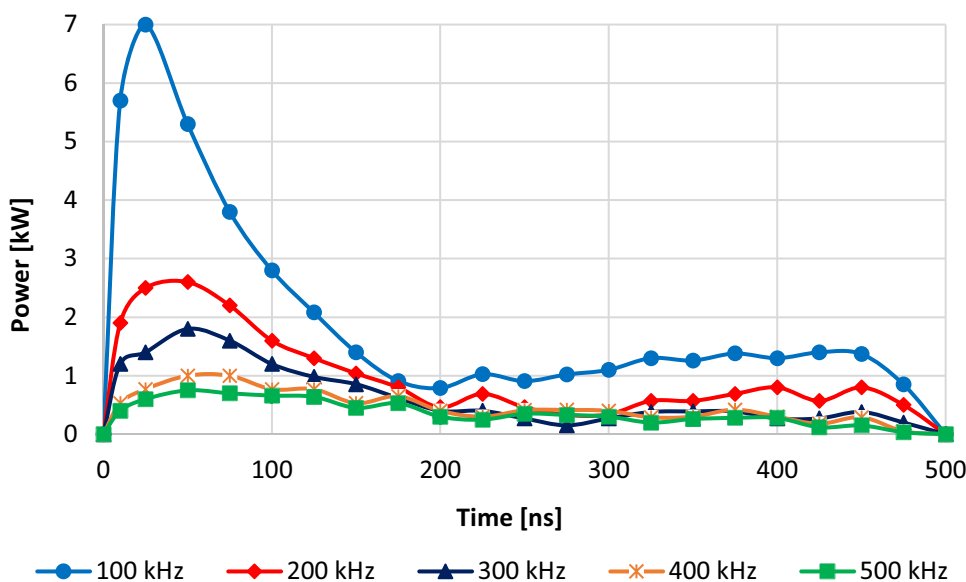

Fig. 1 Thermal cycle in CW mode

Fig. 2 Thermal cycle in millisecond SPPW mode

Fig. 3 Nanosecond MPPW laser temporal response for different pulse repetition frequencies at a constant average power of 100 W [25]

the calculation of the pulse energy, as if the pulse shape was always square for any frequency. Therefore, the average peak power (P_{peak}) of the nanosecond MPPW laser is normally lower than the peak power, but higher than the average power [25].

Both the average power and average peak power play an important role in the weld shape of MPPW welding, and the process is controlled through the average power density, like CW mode in Eq. (1), and the average peak power density ($q_{p,\,peak}$), as given in Eq. (3) [25]:

$$q_{p,peak} = P_{peak}/A_s (MW/cm^2) \qquad (3)$$

There are several factors affecting the overlap between pulses in MPPW welding, and consequently, the thermal losses. First, the inter-pulse spacing increases as the frequency and the laser duty cycle decrease, as shown by Eq. (4), with the thermal losses more significant in this regime:

$$I_s = (1 - DC)/PRF (\mu s) \qquad (4)$$

Second, the higher the energy delivered in several consecutive pulses, the longer it takes for the material to cool down back to room temperature, even if the overlap between pulses is close. Third, the thermal losses will be lower if the same energy is delivered faster to the material. And fourth, the physical properties of the processed material will affect the thermal losses since the time for the heat to diffuse over a unit distance, referred to as characteristic length, depends on the material's thermal diffusivity (α) and is quantified by the characteristic thermal time t_0 [26], as given by Eq. (5). The MPPW laser welding regime features energy accumulation between pulses, as represented by the thermal cycle in Fig. 4:

$$t_0 = d^2/16\alpha (s) \qquad (5)$$

2.3 Laser-material interaction times for different operating modes

To compare CW and PW processes, we need to have a way of converting travel speed from CW to time-domain of pulse duration from PW. Interaction time, a discrete unit time, can be used for this purpose. For CW mode, the laser-material interaction time ($t_{i,\,CW}$) is represented by the ratio of the beam diameter (d) in welding direction to the travel speed (v), as given by Eq. (6):

$$t_{i,CW} = d/v (ms) \qquad (6)$$

The laser-material interaction time in single-pulse PW mode ($t_{i,\,SPPW}$) is equal to the pulse duration, as given by Eq. (7):

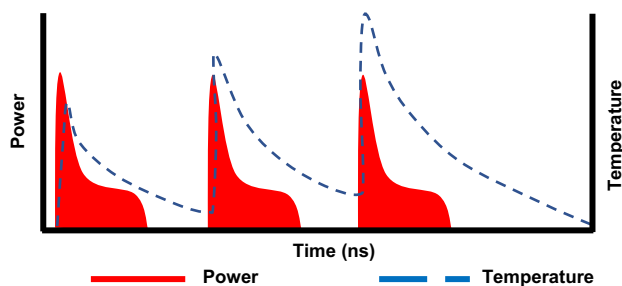$$t_{i,SPPW} = P_{Width} (ms) \qquad (7)$$

Fig. 4 Thermal cycle in nanosecond MPPW mode

However, in MPPW processing, the pulse duration needs to be converted back into the space domain where cumulative exposure time of multiple spots over a unit length can be calculated. This should consider the overlap factor and the gap between individual pulses. In a definition proposed by Banat et al. [21], interaction time in MPPW mode ($t_{i,\,MPPW\,(old)}$) represents the summation of the duration of each emitted pulse with a certain overlap factor (O_F), as given by Eqs. (8) and (9), respectively. At 0% overlap factor, the interaction time is equal to pulse width, and at 100%, the equation is not applicable since the beam is stationary:

$$t_{i,\,MPPW(old)} = P_{Width}/(1 - O_F/100)\,(ms) \qquad (8)$$

$$O_F = \left(1 - \frac{v}{dPRF}\right)100\,(\%) \qquad (9)$$

In Eq. (9), it is possible to have the same overlap factor achieved at different processing speeds, hence different frequencies, and in such a case, the inter-pulse spacing will be different. The laser-material interaction time in Eq. (8) does not capture the thermal losses created by the inter-pulse spacing and material properties. A new definition that captures global losses due to processing speed and thermal losses due to the absence of power in between the pulses is proposed in Eq. (10), the new MPPW interaction time ($t_{i,\,MPPW\,(new)}$). If there is no inter-pulse spacing, $t_{i,\,MPPW\,(new)}$ is equal to the ratio between beam diameter and travel speed, like in Eq. (6) for CW mode. The larger the beam diameter used, the longer the characteristic thermal time, being smaller the ratio between I_s and t_0. This ratio also gets smaller for short inter-pulse spacing, and in both cases, $t_{i,\,MPPW\,(new)}$ approximates to the normal definition of $t_{i,\,CW}$ in Eq. (6) for CW mode. The overall

effective applied energy in MPPW welding delivered for a certain interaction time is given by Eq. (11):

$$t_{i,\,MPPW\,(new)} = (d/v)/(1 + I_s/t_0)\,(ms) \qquad (10)$$

$$E_{SP,\,MPPW\,(new)} = q_p t_{i,\,MPPW\,(new)}\,A_S = P_L t_{i,\,MPPW\,(new)}\,(J) \qquad (11)$$

From Figs. 5 to 7 are compared the two different definitions of interaction time for MPPW mode, the old definition proposed by Banat et al. [21] and the new definition proposed in this paper, and a standard definition from CW mode. Figure 5 shows the effect of different travel speeds on $t_{i,\,CW}$ at a constant beam diameter, and on $t_{i,\,MPPW\,(new)}$ and $t_{i,\,MPPW\,(old)}$ at a constant overlap factor, beam diameter and pulse width. As the travel speed increases, $t_{i,\,MPPW\,(new)}$ and $t_{i,\,CW}$ decrease. The overlap between pulses is kept constant as $t_{i,\,MPPW\,(new)}$ decreases since the frequency increases in the same proportion of travel speed. However, for similar travel speed, $t_{i,\,MPPW\,(new)}$ begins at a higher value than $t_{i,\,MPPW\,(old)}$ as it allows for energy accumulation between pulses and consequently, reduction of thermal losses. Thus, the new definition $t_{i,\,MPPW\,(new)}$ approaches that of $t_{i,\,CW}$ much more quickly since the gap between pulses decreases. As the travel speed becomes higher, the difference between $t_{i,\,MPPW\,(new)}$, $t_{i,\,MPPW\,(old)}$ and $t_{i,\,CW}$ becomes much smaller. The $t_{i,\,MPPW\,(old)}$ remains constant and below the other two definitions as it only considers the summation of pulses delivered in a certain spatial domain, without capturing either the inter-pulse spacing or the material properties' effects on the heat accumulation. Therefore, the ratio between inter-pulse spacing and the characteristic thermal time from $t_{i,\,MPPW\,(new)}$ in Eq. (10) represents the local thermal losses characteristic from MPPW operation lasers.

Fig. 5 Interaction times versus travel speed for a constant overlap factor of 99%, beam diameter of 35 μm and pulse width of 500 ns
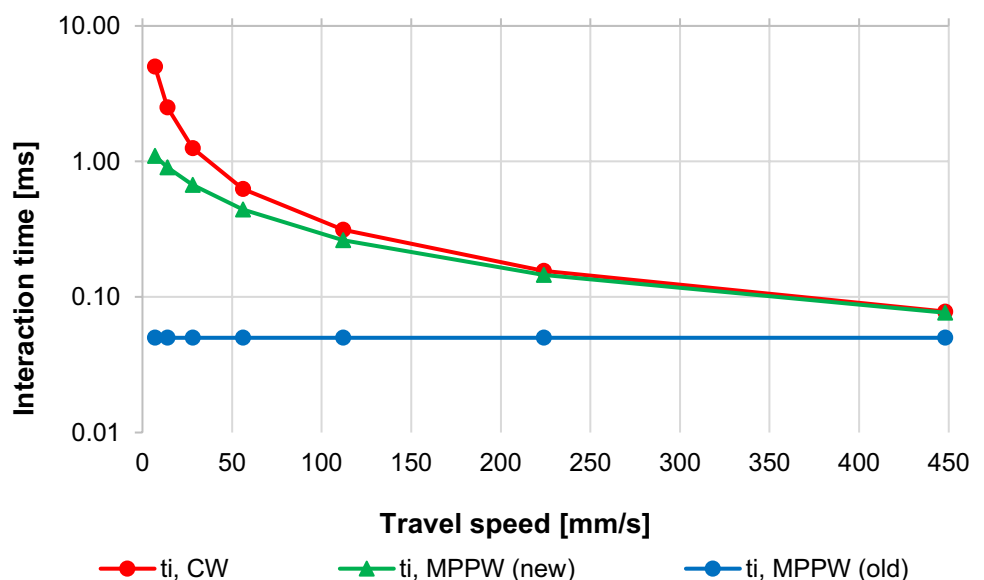
Fig. 6 Interaction times versus travel speed for a constant frequency of 100 kHz, beam diameter of 35 μm and pulse width of 500 ns
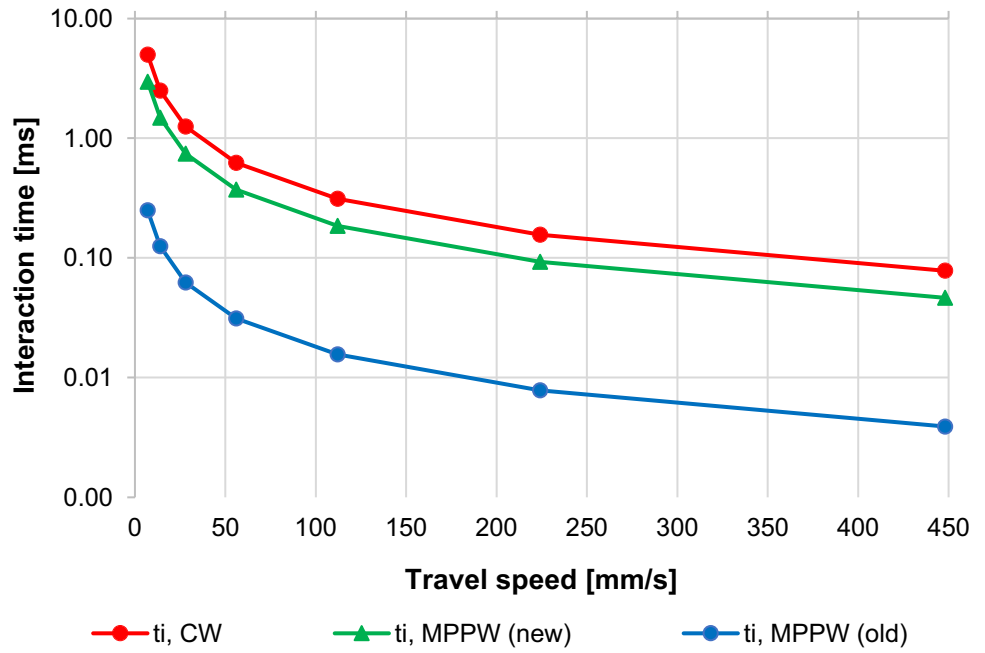

Figure 6 shows the effect of different travel speeds on $t_{i,\,CW}$ at a constant beam diameter, and on $t_{i,\,MPPW\,(new)}$ and $t_{i,\,MPPW\,(old)}$ at a constant frequency, beam diameter and pulse width. All interaction times decrease as the travel speed increases, being the global thermal losses similar in CW and MPPW modes for similar speeds. As the pulse width and frequency are constant, the inter-pulse spacing does not change. Therefore, the gap between $t_{i,\,MPPW\,(new)}$, $t_{i,\,MPPW\,(old)}$ and $t_{i\,CW}$ is constant since the local thermal losses caused by the constant inter-pulse spacing are similar.

In Fig. 7, $t_{i,\,CW}$ is insensitive to the frequency of pulsing hence is constant for constant processing speed. It considers global thermal losses which are dependent on processing speed and material thermal properties. The $t_{i,\,MPPW\,(old)}$ and $t_{i,\,MPPW\,(new)}$ increase as the frequency increases at a constant travel speed, increasing the overlap factor in the same proportion. However, for similar frequency, $t_{i,\,MPPW\,(new)}$ begins at a higher value than $t_{i,\,MPPW\,(old)}$ as it allows for energy accumulation between pulses and, consequently, reduction of thermal losses. Therefore, as also previously observed in Fig. 5, the new definition $t_{i,\,MPPW\,(new)}$ approaches that of $t_{i,\,CW}$ much more quickly in Fig. 7 since it considers once again the reduction of inter-pulse spacing for higher frequencies.

Fig. 7 Interaction times versus frequency for a constant travel speed of 56 mm/s, beam diameter of 35 μm and pulse width of 500 ns
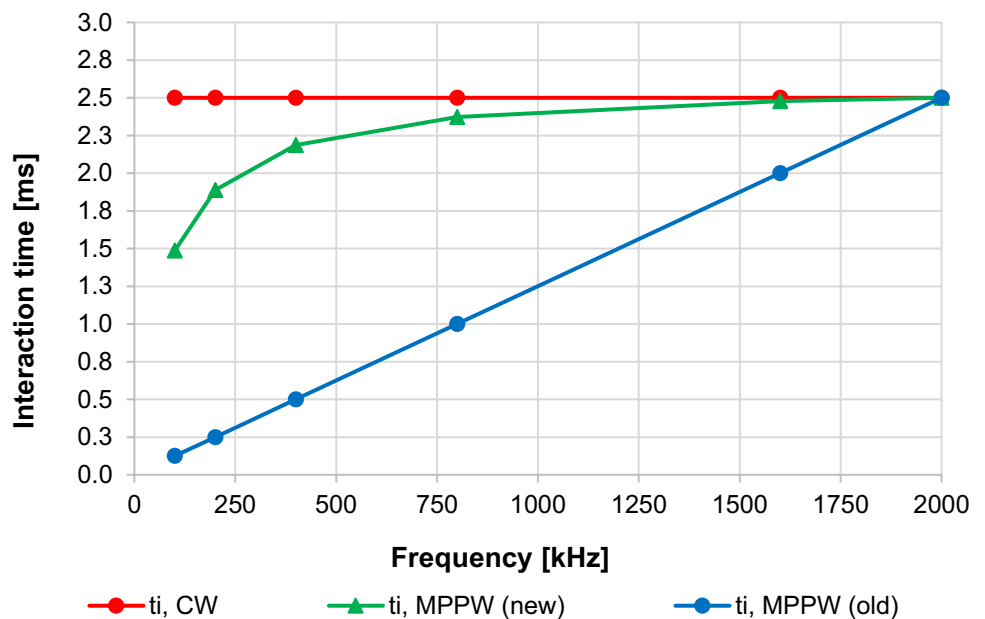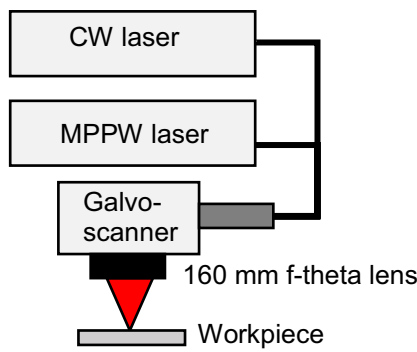
Fig. 8 Experimental setup of MPPW and CW fibre lasers used for stainless-steel welding

Fig. 9 Pulse shapes of waveforms 0 and 31 at PRF_0 of 100 kHz

3 Experimental procedure

Bead-on-plate welds were carried out in 304L austenitic stainless steel with the following dimensions: $40 \times 70 \times 2$ mm ($W \times L \times D$). The experimental setup is shown in Fig. 8. Welding experiments were performed with two different TRUMPF fibre lasers: a 500-W average power CW laser and a 100-W average power nanosecond MPPW laser (1060–1080 nm wavelength). Both lasers were integrated with the same optics (galvo scanning optics by RAYLASE), and the same spot sizes were achieved. The laser power was measured and calibrated by a Laserpoint power meter, and the beam profiles were measured using a DataRay slit-scan beam profiler. The temporal response of the PW laser radiation was measured using a high-speed photodetector (MenloSystems) connected to an oscilloscope (Tektronix) with 1 GHz bandwidth and a sampling capacity of 5 Giga samples per second (Gs/s). This laser can deliver different pulse shapes, referred to as pre-programmed waveforms.

The nanosecond MPPW laser used in this study allows the selection of 31 different waveforms. For instance, waveform 0 is characterised by a pulse width of 280 ns, peak power of 10 kW and pulse energy of 1 mJ. On the other hand, waveform 31 has the longest pulse duration of 500 ns, peak power of 7 kW and pulse energy of 1 mJ. The pulse shapes of both waveforms are shown in Fig. 9 at a PRF_0 of 100 kHz. Only waveform 31 was selected to be explored in this work, as shown in Table 2.

An air knife was used with compressed gas to protect the 160-mm f-theta focusing lens from spatter, and no shielding gas was applied on the substrate. Before welding, the base materials were groun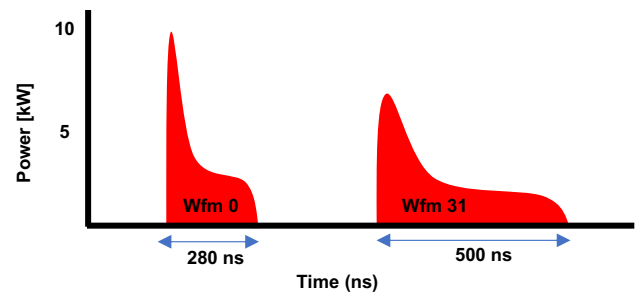d to remove any oxide layers or residues and cleaned with acetone. All the produced welds were mounted in plastic moulds using an epoxy resin mixed with a hardener. The samples were mechanically ground, polished and electrolytically etched with 10% of oxalic acid to reveal the microstructure of stainless steel. Micrographs were taken with an Optiphot optical microscope with total magnification ranging from $2.5 \times$ to $40 \times$. The experimental error was calculated based on the difference of the weld shape, i.e. penetration depth and weld width, measured between the first and second cross-sections at the beginning and end of the 40-mm-long weld seam for the same processing conditions. The welds with an experimental error above 10% were excluded from the analysis of the results.

4 Methodology

4.1 Comparison of MPPW to CW welding at different processing conditions

MPPW laser allows high peak power applied at high frequency (kHz), generating energy accumulation, and melting from a certain overlap between pulses. On the other hand, CW laser is characterised by a higher average power and lower peak power than MPPW. Therefore, MPPW mode was compared to CW at different parameter ranges in different case studies.

4.1.1 Constant overlap factor

This section aims to investigate the effect of the MPPW laser's inter-pulse thermal losses on the weld shape, i.e. penetration depth and width, penetration and melting efficiency and to make a comparison with CW welds under

Table 2 Characteristics of waveform 31 of MPPW laser [27]

Waveform	PRF_0 (kHz)	Max pulse energy, Emax (mJ)	Pulse width (ns)	Peak Power at Emax (kW)
31	100	1	500	7

similar processing conditions. The penetration efficiency (P_{Eff}) was calculated as the ratio between the total applied energy (E_{SP}) and penetration depth (P_{Depth}), as given by Eq. (12). The melting efficiency (M_{Eff}) was calculated as the ratio between E_{SP} and the product between the area of the weld cross-section (A_{CS}) and weld length (W_L), as given by Eq. (13):

$$P_{Eff} = E_{SP}/P_{Depth}(\text{J/mm}) \tag{12}$$

$$M_{Eff} = E_{SP}/(A_{CS} \times W_L)(\text{J/mm}^3) \tag{13}$$

A constant overlap factor of 99% was used in MPPW mode, and a similar range of travel speeds from 32 to 140 mm/s, average power and beam diameter was applied in both temporal modes. The average power density was kept similar in both laser modes, and the average peak power density and applied energy were varied in MPPW mode through different pulse repetition frequencies. The set of parameters used is shown in Table 3.

4.1.2 Constant frequency

At constant frequency and lower travel speed, the delivered energy by the MPPW laser can equal that of the CW laser. This section aims to investigate the effect of the MPPW laser's processing speed on the weld shape, penetration and melting efficiency and to make a comparison with CW welds at similar energy levels. A constant frequency of 400 kHz was used in MPPW mode, and similar average peak power and beam diameter were applied in both temporal modes. The average peak power density and applied energies were kept similar in both lasers. The set of parameters used is shown in Table 4.

5 Results and discussion

5.1 Comparison of MPPW to CW welding at different processing conditions

Normally, when using system parameters, the MPPW process would have specified pulse duration and overlap factor, whilst the processing speed would be selected in CW. From the perspective of material, it should be able to describe how much energy is applied per unit length for both processes to achieve similar weld shapes. The current laser welding definitions do not allow a direct comparison between MPPW and CW modes. This section focuses on the comparison of a new set of proposed definitions for MPPW mode with the conventional fundamental laser-material interaction parameters (FLMIPs) already established in CW mode [23].

Table 3 MPPW and CW welding parameters at a similar range of travel speeds, average power, beam diameter and constant overlap factor of 99% in MPPW

MPPW laser

Fundamental laser material interaction parameters				System parameters						Calculated Parameters	
$q_{p,peak}$ [MW/cm²]	q_p [MW/cm²]	$E_{SP, MPPW (new)}$ [mJ]	$t_{i,MPPW (new)}$ [ms]	PRF [kHz]	v [mm/s]	d [μm]	P_L [W]	E_{pulse} [mJ]	P_{peak} [W]	O_F [%]	I_s [μs]
208	**10.4**	59	0.59	100	**35**	**35**	**100**	1.0	2000	99	10
104	**10.4**	38	0.38	200	**70**	**35**	**100**	0.50	1000	99	5
52	**10.4**	22	0.22	400	**140**	**35**	**100**	0.25	500	99	2

CW laser

| Fundamental laser material interaction parameters			System parameter		
q_p [MW/cm²]	$E_{SP, cw}$ [mJ]	$t_{i, cw}$ [ms]	v [mm/s]	d [μm]	P_L [W]
10.4	100	1.0	**35**	**35**	**100**
10.4	50	0.5	**70**	**35**	**100**
10.4	25	0.25	**140**	**35**	**100**

Similar parameters used in both MPPW and CW lasers are shown in bold

Table 4 MPPW and CW welding parameters at a similar average peak power, beam diameter and constant frequency of 400 kHz in MPPW

MPPW laser

Fundamental laser material interaction parameters				System parameters						Calculated Parameters	
$E_{SP, MPPW \, (new)}$ [mJ]	$t_{i, MPPW \, (new)}$ [ms]	$q_{p, peak}$ [MW/cm²]	q_p [MW/cm²]	v [mm/s]	d [µm]	P_L [W]	PRF [kHz]	E_{pulse} [mJ]	P_{peak} [W]	O_F [%]	I_s [µs]
25	0.25	**8.0**	1.6	356	**89**	100	400	0.25	**500**	99.0	2
125	1.25	**8.0**	1.6	71	**89**	100	400	0.25	**500**	99.8	2
250	2.5	**8.0**	1.6	35	**89**	100	400	0.25	**500**	99.9	2
500	5.0	**8.0**	1.6	17	**89**	100	400	0.25	**500**	99.95	2
1000	10	**8.0**	1.6	9	**89**	100	400	0.25	**500**	99.97	2

CW laser

Fundamental laser material interaction parameters			System parameters		
$E_{SP, \, cw}$ [mJ]	$t_{i,cw}$ [ms]	$q_{p,}$ [MW/cm²]	v [mm/s]	d [µm]	P_L [W]
25	0.050	**8.0**	1756	**89**	**500**
125	0.25	**8.0**	356	**89**	**500**
250	0.50	**8.0**	178	**89**	**500**
500	1.0	**8.0**	89	**89**	**500**
1000	2.0	**8.0**	45	**89**	**500**

Similar parameters used in both MPPW and CW lasers are shown in bold

Fig. 10 Depth of penetration in CW and MPPW laser welding at an average power of 100 W, beam diameter of 35 μm and overlap factor of 99% in MPPW
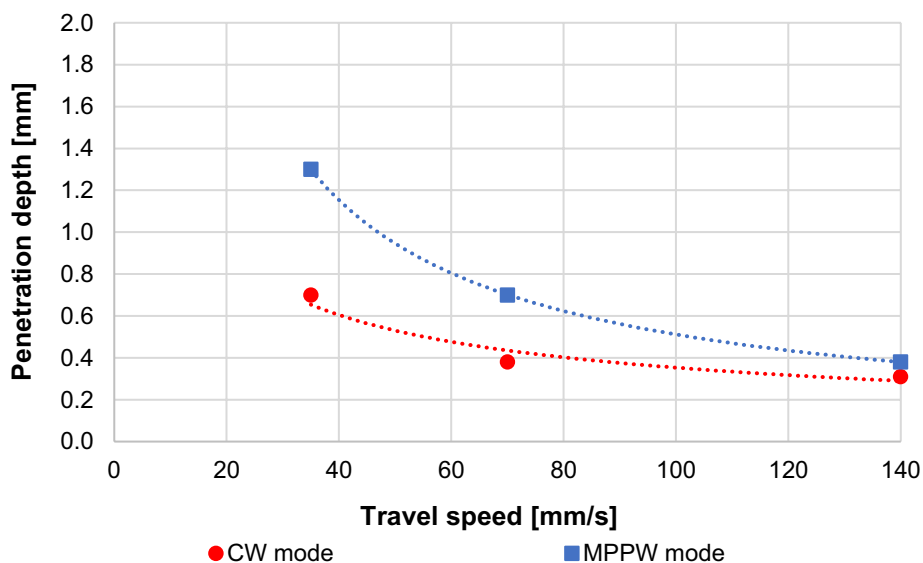
5.1.1 Constant overlap factor
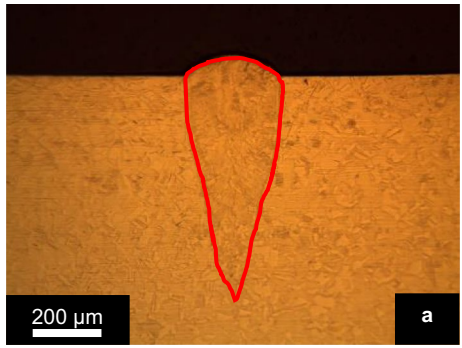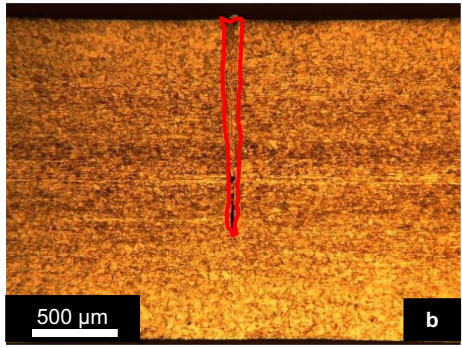
If we neglect the high peak power and frequency of the MPPW laser, then it can be treated almost as a CW laser, and a direct comparison can be made. In Figs. 10 and 11, both lasers were compared at the same average power, travel speed and spot size. The MPPW laser gives higher penetration, but the weld profiles compared in Fig. 11 show that CW welds are much wider than in MPPW. As the travel speed increases at a constant overlap factor, the weld width remains relatively constant in MPPW, with a slight deviation at 140 mm/s, but it decreases in CW mode eventually to reach the same low weld width as in MPPW mode. Therefore, in theory, the weld width should not change at all as the travel speed is increasing, and

the pulse energy is decreasing. Nevertheless, from 35 to 140 mm/s, the weld width of the MPPW laser is almost constant in comparison to CW, and for 140 mm/s, it is still within the experimental error.

The micrographs of each temporal mode from Figs. 10 and 11 are shown in Figs. 12 and 13. In Fig. 12, the global thermal losses are the same in both laser modes since the travel speed is the same, but the duty cycle of the MPPW laser is much less than the 100% in CW laser. Therefore, both the new and old definitions of interaction time capture this and explain the difference in weld width. The penetration depth is higher in MPPW mode (Fig. 12b) due to the much higher average peak power density, which overtakes the local thermal losses responsible for lower interaction time.

Fig. 11 Weld width in CW and MPPW laser welding at an average power of 100 W, beam diameter of 35 μm and constant overlap factor of 99% in MPPW
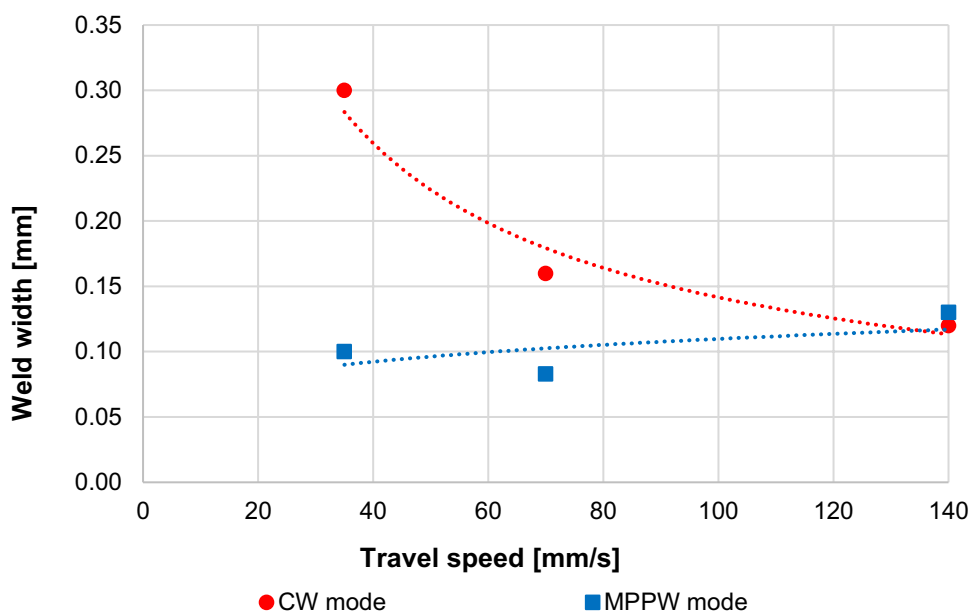
Fig. 12 CW and MPPW welds (weld boundaries delimited in red) at a travel speed of 35 mm/s, average power of 100 W, beam diameter of 35 μm and constant overlap factor of 99% in MPPW
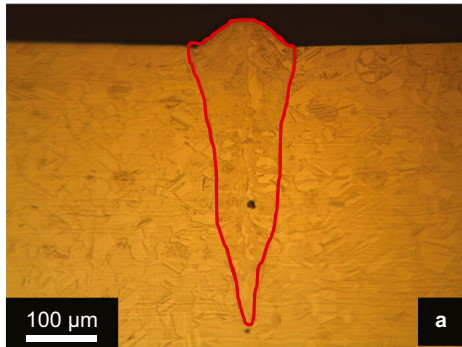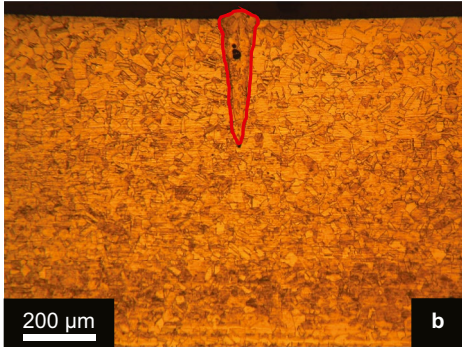

$v = 35$ mm/s; $P_L = 100$ W; $d = 35$ μm	
CW mode	**MPPW mode**
$q_p = 10.4$ MW/cm^2	$q_{p,\ peak} = 208$ MW/cm^2; $q_p = 10.4$ MW/cm^2
$E_{SP,\ cw} = 100$ mJ	$E_{SP,\ MPPW\ (new)} = 59$ mJ; $E_{SP,\ MPPW\ (old)} = 100$ mJ
$t_{i,\ cw} = 1$ ms	$t_{i,\ MPPW\ (new)} = 0.59$ ms; $t_{i,\ MPPW\ (old)} = 0.05$ ms
Depth = 0.7 mm; Weld width = 0.3 mm	Depth = 1.3 mm; Weld width = 0.11 mm
Weld metal area = 0.12 mm^2	Weld metal area = 0.069 mm^2

From Figs. 12 to 13, the CW and MPPW lasers behave as normal, reducing the penetration depth with travel speed due to an energy reduction. Despite the five times higher average peak power density in MPPW laser in Fig. 13b, the penetration depth is almost the same as in CW laser in Fig. 13a. This means that it is not the average peak power density, but the frequency and hence inter-pulse thermal losses that are important. In this regime, the pulse energy of individual pulses is too low to generate melting, and more pulses are needed to initiate melting at a constant overlap factor; hence, the thermal losses are more important than the peak power density of individual pulses. On the other hand, fewer pulses are needed to generate melting in Fig. 12b due to the higher energy per pulse, but the higher inter-pulse spacing and travel speed generated higher thermal losses than in Fig. 13b, which explains the similar weld widths in both cases.

The inter-pulse thermal losses are captured by the proposed new definition of interaction time. From Figs. 12

Fig. 13 CW and MPPW welds (weld boundaries delimited in red) at a travel speed of 140 mm/s, average power of 100 W, beam diameter of 35 μm and constant overlap factor of 99% in MPPW

$v = 140$ mm/s; $P_L = 100$ W; $d = 35$ μm	
CW mode	**MPPW mode**
$q_{p,\ peak} = 10.4$ MW/cm^2	$q_{p,\ peak} = 52$ MW/cm^2; $q_{p,\ peak} = 10.4$ MW/cm^2
$E_{SP,\ cw} = 25$ mJ	$E_{SP,\ MPPW\ (new)} = 22$ mJ; $E_{SP,\ MPPW\ (old)} = 25$ mJ
$t_{i,\ cw} = 0.25$ ms	$t_{i,\ MPPW\ (new)} = 0.22$ ms; $t_{i,\ MPPW\ (old)} = 0.05$ ms
Depth = 0.31 mm; Weld width = 0.12 mm	Depth = 0.38 mm; Weld width = 0.13 mm
Weld metal area = 0.024 mm^2	Weld metal area = 0.029 mm^2

Fig. 14 Energy to penetrate 1 mm of metal in CW and MPPW laser modes at an average power of 100 W, beam diameter of 35 μm and constant overlap factor of 99% in MPPW
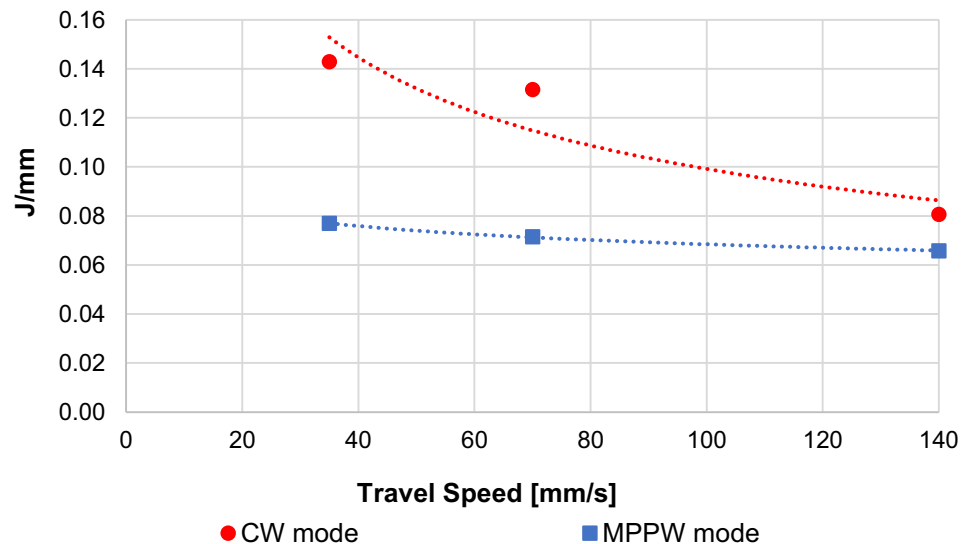
to 13, $t_{i, MPPW (new)}$ is much closer to $t_{i, CW}$, being the thermal losses similar. On the other hand, $t_{i, MPPW (old)}$ remained unchanged and below $t_{i, MPPW (new)}$ and $t_{i, CW}$ being unable to capture the effect of pulse spacing reduction on the weld shape. This observation agrees with the research hypothesis previously explained in Fig. 5.

The penetration and melting efficiencies from Figs. 10 and 11 are shown in Figs. 14 and 15, respectively. In MPPW mode, the higher peak power opens the keyhole more easily, allowing a higher penetration efficiency than in CW mode for similar travel speeds, as observed in Fig. 14. However, as the frequency increases in the same proportion of travel speed to keep the overlap factor constant, the inter-pulse spacing decreases in MPPW mode, decreasing the thermal losses between pulses as well. Thus, the penetration efficiency converges in both temporal modes as the travel speed increases due to an approximation of $t_{i, CW}$ and $t_{i, MPPW (new)}$, as previously explained in Fig. 5.

The melting efficiency of both laser modes is shown in Fig. 15. For similar energy and travel speed, MPPW laser requires more energy than CW laser to melt 1 mm^3 of metal. As the travel speed increases, the energy required by CW mode increases slightly since the welds become narrower and shallower. On the other hand, in MPPW mode, the weld width remains constant, but the penetration depth decreases, being the weld aspect ratio always higher than in CW mode. Both the melting and penetration efficiencies converge in both temporal modes as the inter-pulse thermal losses decrease and become similar for higher travel speeds and frequencies, which validates the research hypothesis proposed in Sect. 2.3.

Fig. 15 Energy to melt 1 mm^3 of metal in CW and MPPW laser modes at an average power of 100 W, beam diameter of 35 μm and constant overlap factor of 99% in MPPW
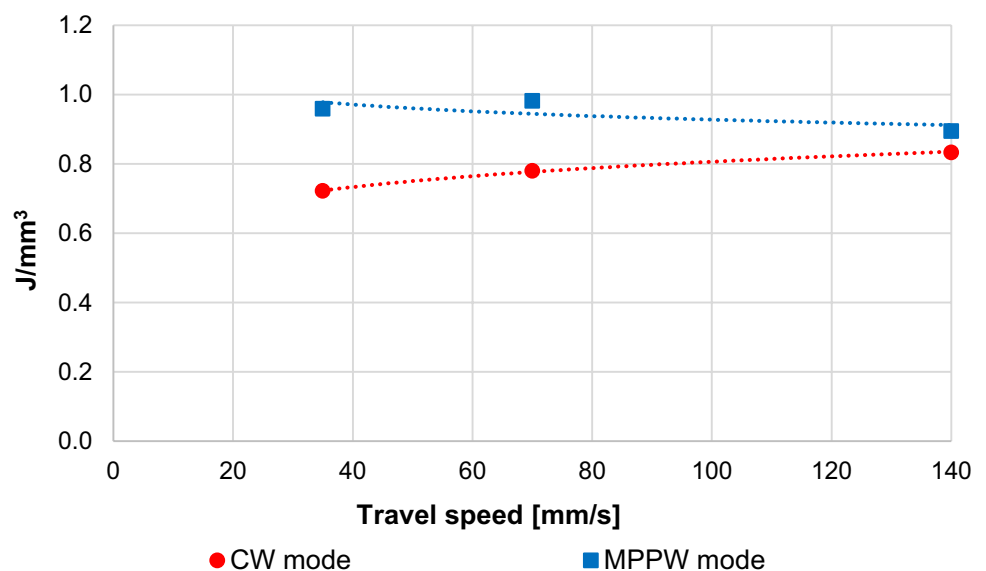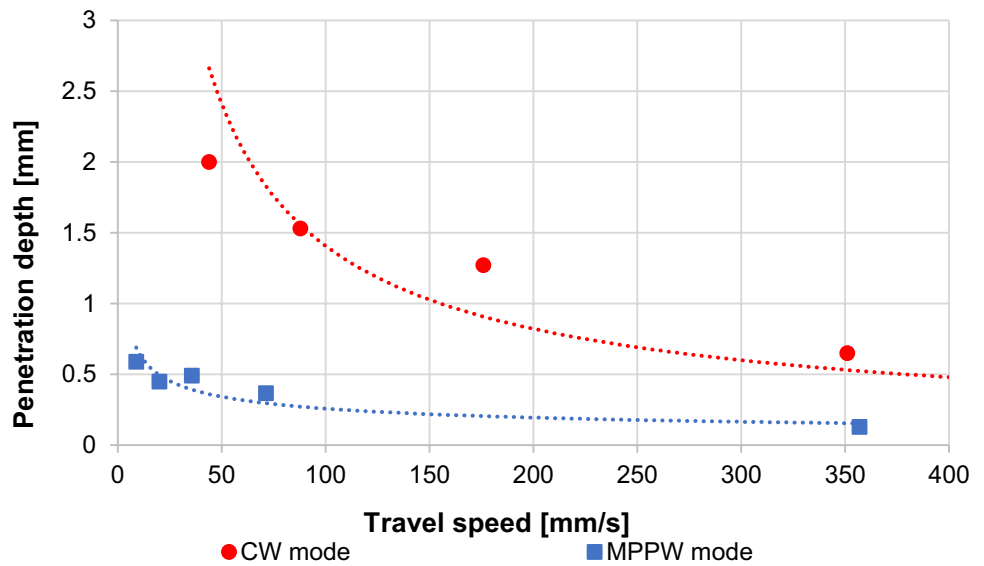
Fig. 16 Depth of penetration in CW and MPPW laser welding at an average peak power of 500 W and a constant frequency of 400 kHz in MPPW

5.1.2 Constant frequency

A comparison between CW and MPPW seam welding is shown in Figs. 16 and 17 at different travel speeds and similar average peak power and beam diameter. As the travel speed increases, the penetration depth and weld width decrease in both welding modes. Since the frequency is kept constant in MPPW mode, the inter-pulse spacing and the energy delivered per pulse remained constant, being the local thermal losses constant as well, as previously explained in Fig. 6.

A micrograph of each temporal mode from Figs. 16 and 17 is shown in Fig. 18. The reduction in travel speed at a constant frequency in MPPW mode allowed energy to build up to the same level as in CW mode. However, it is shown in Fig. 18b for MPPW laser that the global thermal

losses are higher in this regime since the penetration depth is shallower, and the weld width is wider than in CW mode in Fig. 18a. This is captured by $t_{i,\ MPPW\ (new)}$ which is much higher than $t_{i,\ CW}$, but not by $t_{i,\ MPPW\ (old)}$, which is equal to $t_{i,\ CW}$. These observations corroborate once again the research hypothesis of this work presented in Sect. 2.3.

The penetration and melting efficiencies from Figs. 16 and 17 are presented in Figs. 19 and 20, respectively. The energy required in MPPW laser to penetrate 1 mm and melt 1 mm^3 of metal is always higher than CW until a certain travel speed, from which both temporal modes start converging, as also observed in the previous section. Due to the lack of average power in MPPW laser in comparison to CW mode, reducing the travel speed to increase $t_{i,\ MPPW\ (new)}$ and consequently achieve similar applied energy is not efficient. For low travel speeds, the thermal losses are more intense in

Fig. 17 Weld width in CW and MPPW laser welding at an average peak power of 500 W and a constant frequency of 400 kHz in MPPW
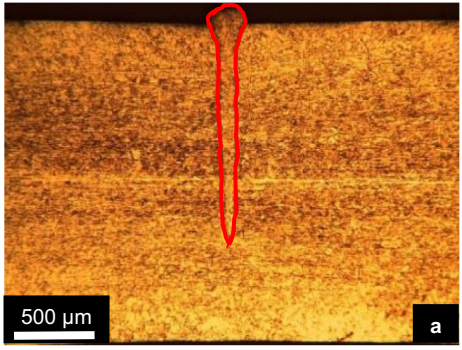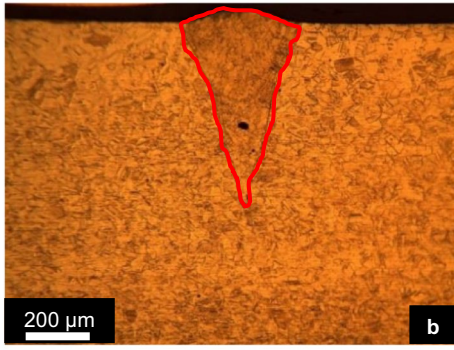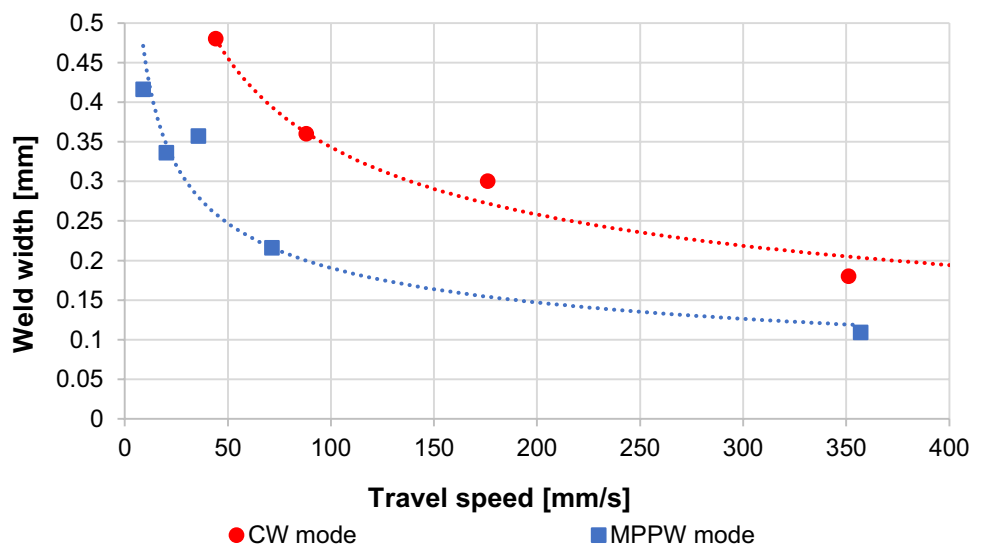
Fig. 18 CW and MPPW welds (weld boundaries delimited in red) at an average peak power of 500 W, beam diameter of 89 μm and a frequency of 400 kHz in MPPW

P_{peak} = 500 W; d = 89 μm	
CW mode	**MPPW mode**
v = 178 mm/s; P_L = 500 W	v = 35.6 mm/s; PRF = 400 kHz; P_L = 100 W
q_p = 8 MW/cm² $E_{SP, cw}$ = 250 mJ	q_p = 1.6 MW/cm²; $q_{p, peak}$ = 8 MW/cm² $E_{SP, MPPW (new)}$ = 250 mJ; $E_{SP, MPPW (old)}$ = 250 mJ
$t_{i, cw}$ = 0.5 ms	$t_{i, MPPW (new)}$ = 2.5 ms; $t_{i, MPPW (old)}$ = 0.5 ms
500 μm (a)	200 μm (b)
Depth = 1.3 mm; Weld width = 0.20 mm Weld metal area = 0.15 mm²	Depth = 0.55 mm; Weld width = 0.29 mm Weld metal area = 0.082 mm²

MPPW mode, and the required energy increases exponentially since the gap between $t_{i, CW}$ and $t_{i, MPPW (new)}$ is much bigger (Table 4). Assuncao and Williams [16] observed opposite results to the ones shown in Fig. 19. According to them, the penetration efficiency is higher in PW than in CW mode. However, they compared spot welds in PW with seam welds in CW mode, which may have had an impact on the results due to the different melt pool dynamics. The PW laser was stationary, and the interaction time was equal to the pulse width, the total energy uniquely delivered in a single spot. On the other hand, the beam in CW mode was in movement, and part of the energy was also used to heat the substrate for a certain weld length, being consequently lost and the penetration depth lower.

In summary, there is a clear difference between laser temporal modes depending on what is being compared. The new set of proposed parameters can capture the thermal losses in MPPW mode, which allows a direct comparison in productivity, penetration and melting efficiency with CW mode. The energy utilised for melting of the material is higher for

Fig. 19 Energy to penetrate 1 mm of metal in CW and MPPW laser modes at an average peak power of 500 W, beam diameter of 89 μm and a constant frequency of 400 kHz in MPPW
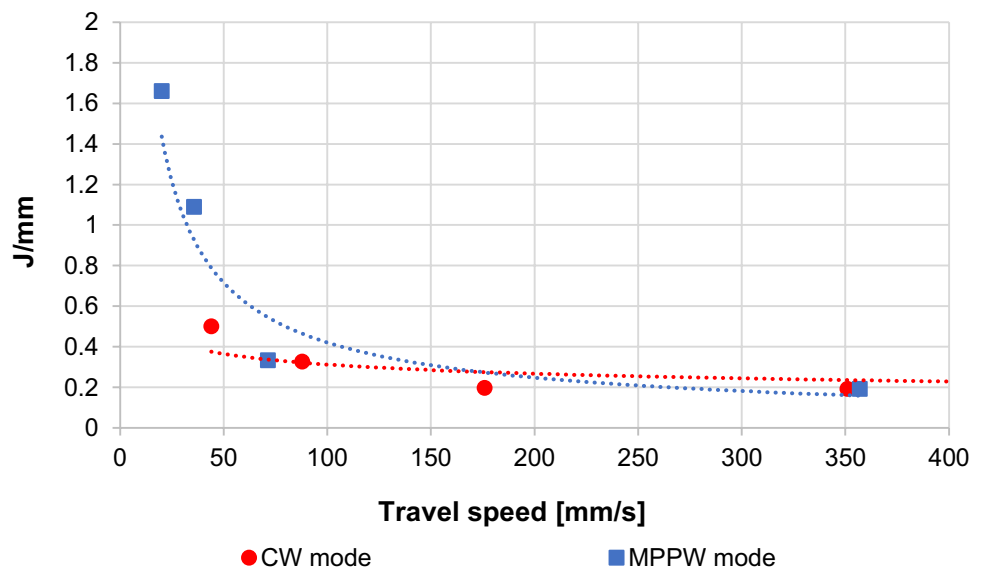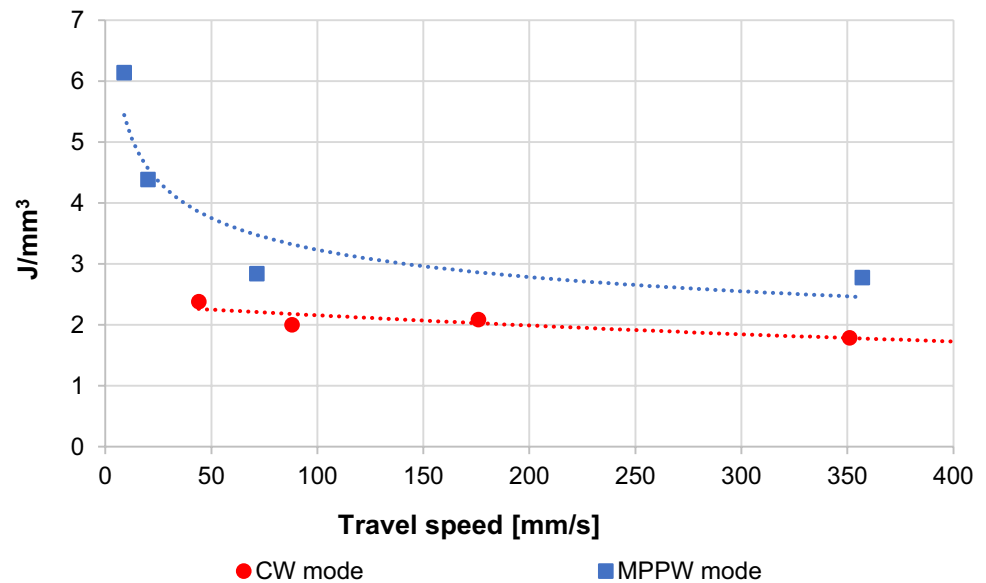
Fig. 20 Energy to melt 1 mm^3 of metal in CW and MPPW laser modes at an average peak power of 500 W, beam diameter of 89 μm and a constant frequency of 400 kHz in MPPW

CW laser because it is operated at optimum parameter range used in micro-welding (high travel speeds and high average power). Therefore, the CW laser allows low thermal losses and its melting efficiency is higher compared to the MPPW laser. The nanosecond MPPW works like ultra-short lasers almost as in a drilling regime [28], generating low melting and high aspect ratio welds, being the penetration efficiency higher than in CW mode. Nevertheless, the new MPPW lasers do not provide the maximum energy for all ranges of frequencies because of the response of the resonator above a certain critical frequency (PRF_0) and pulse duration. The pulse energy and peak power are higher for lower frequencies closer to PRF_0, but the inter-pulse spacing is longer, increasing the thermal losses between pulses and the required energy to achieve deeper and wider welds. On the other hand, for high frequencies above PRF_0, the pulse energy and peak power are decreased to avoid overheating of the diodes, and the pulse shape becomes almost flat, decreasing the energy available to penetrate and melt more metal. Therefore, the lower average power of the MPPW laser in comparison to CW laser is its biggest limitation, providing lower melting efficiency regardless of the frequency or travel speed used. Using the new set of proposed parameters, similar weld shapes, i.e. penetration depths and weld widths, can only be achieved in both temporal modes for similar average power density, specific point energy and interaction time. The benefit of the much higher average peak power density of the MPPW laser is only relevant for very specific applications where high aspect ratio welds and low heat input are required to minimise the heat-affected zone, such as in the manufacturing of biomedical devices, orthopaedic and prosthetics [29]. However, if the application requires high productivity and good fit-up tolerance, such as welding of battery packs

for electric vehicles [30], then the advantage of the higher average power available in the CW laser must be utilised, providing superior performance than the MPPW laser.

6 Conclusions

CW and MPPW laser processing modes showed different interactions with the material in micro-seam welding. Comparing both processes, the following conclusions can be drawn:

– It is possible to compare both modes considering the energy applied to the material.
– The inter-pulse spacing is as important as the overlap factor in MPPW mode.
– A new definition of interaction time has been proposed, tested and validated to enable like-for-like comparison with CW mode by capturing the thermal losses effect on the weld shape.
– For similarly applied energies, the average peak power density in MPWW mode can be neglected. Several pulses are needed to initiate melting at a constant overlap factor; hence, the thermal losses are more important than the high peak power of an individual pulse.
– Similar weld shapes (penetration depth and weld width) can only be achieved in both modes if similar average power density, specific point energy and interaction time are applied.
– The penetration efficiency of the MPPW laser is only higher than CW for low frequencies. However, the melting efficiency of the MPPW laser is lower.

– The melting and penetration efficiency of the MPPW laser converge with CW as the thermal losses become similar for high travel speeds and low inter-pulse spacing.
– Further investigation using different materials and the pulse power factor model [25] is recommended to predict the weld shape in MPPW welding using the set of new parameters proposed in this work. Mechanical tests are also recommended to compare the behaviour of both CW and MPPW welds at different processing conditions.

Availability of data and material Not applicable.

Code availability Not applicable.

Declarations

Ethics approval To the author's knowledge, this is the first paper using a set of fundamental parameters to capture thermal behaviour due to the laser temporal mode and material properties. The authors confirm that this manuscript has not been published elsewhere and is not under consideration by another journal. The publication of this manuscript has also been approved by all the co-authors.

Consent to participate Not applicable.

Consent for publication The author transfers to Springer (respective to owner if other than Springer and for U.S. government employees: to the extent transferable) the non-exclusive publication rights and he warrants that his contribution is original and that he has full power to make this grant. The author accepts responsibility for releasing this material on behalf of any and all co-authors. This transfer of publication rights covers the non-exclusive right to reproduce and distribute the article, including reprints, translations, photographic reproductions, microform, electronic form (offline, online) or any other reproductions of similar nature. The author may self-archive an author-created version of his article on his own website and his institution's repository, including his final version; however, he may not use Springer's PDF version which is posted on www.springerlink.com. Furthermore, the author may only post his version provided acknowledgement is given to the Journal and Springer as one of the original places of publication and a link is inserted to the published article on Springer's website.

References

1. Sakagawa T, Nakashiba SI, Hiejima H (2011) Laser micro welding system and its application to seam welding of rechargeable battery. Phys Procedia 12:6–10. https://doi.org/10.1016/j.phpro.2011.03.002
2. Geoffray I, Bourdenet R, Theobald M (2011) Laser micro-welding applied to target manufacturing. Phys Procedia 12:366–372. https://doi.org/10.1016/j.phpro.2011.03.145
3. Patschger A, Bliedtner J, Bergmann JP (2014) Process-limiting factors and characteristics of laser-based micro welding. Phys Procedia 56:740–749. https://doi.org/10.1016/j.phpro.2014.08.081
4. Coroado J, Ganguly S, Williams S et al (2021) Comparison of continuous and pulsed wave lasers in keyhole welding of stainless-steel to aluminium. Int J Adv Manuf Technol. https://doi.org/10.1007/s00170-021-08226-5
5. Pardal G, Meco S, Dunn A et al (2017) Laser spot welding of laser textured steel to aluminium. J Mater Process Technol 241:24–35. https://doi.org/10.1016/j.jmatprotec.2016.10.025
6. Patschger A, Bliedtner J, Bergmann JP (2013) Approaches to increase process efficiency in laser micro welding. Phys Procedia 41:592–602. https://doi.org/10.1016/j.phpro.2013.03.121
7. Biffi CA, Fiocchi J, Bassani P, Tuissi A (2018) Continuous wave vs pulsed wave laser emission in selective laser melting of AlSi10Mg parts with industrial optimized process parameters: microstructure and mechanical behaviour. Addit Manuf. https://doi.org/10.1016/j.addma.2018.10.021
8. Quintino L, Costa A, Miranda R et al (2007) Welding with high power fiber lasers - a preliminary study. Mater Des 28:1231–1237. https://doi.org/10.1016/j.matdes.2006.01.009
9. He X, Fuerschbach PW, DebRoy T (2003) Heat transfer and fluid flow during laser spot welding of 304 stainless steel. J Phys D Appl Phys 36:1388–1398. https://doi.org/10.1088/0022-3727/36/12/306
10. Baruah M, Bag S (2017) Influence of pulsation in thermo-mechanical analysis on laser micro-welding of Ti6Al4V alloy. Opt Laser Technol 90:40–51
11. Assuncao E, Williams S (2014) Effect of material properties on the laser welding mode limits. J Laser Appl 26:012008. https://doi.org/10.2351/1.4826153
12. Torkamany MJ, Tahamtan S, Sabbaghzadeh J (2010) Dissimilar welding of carbon steel to 5754 aluminum alloy by Nd:YAG pulsed laser. Mater Des 31:458–465. https://doi.org/10.1016/j.matdes.2009.05.046

13. Kuo TY, Lin HC (2006) Effects of pulse level of Nd-YAG laser on tensile properties and formability of laser weldments in automotive aluminum alloys. Mater Sci Eng A 416:281–289. https://doi.org/10.1016/j.msea.2005.10.041

14. Okon P, Dearden G, Watkins K et al (2002) Laser welding of aluminium alloy 5083. Proc Int Congr Appl Lasers Electro-Optics (Laser Inst Am 2002) 54:258. https://doi.org/10.1017/CBO9781107415324.004

15. Mizutani M, Yamaguchi Y, Katayama S (2008) Fatigue properties of laser weld in aluminium alloy. Weld Int 22:705–711. https://doi.org/10.1080/09507110802465076

16. Assuncao E, Williams S (2013) Comparison of continuous wave and pulsed wave laser welding effects. Opt Lasers Eng 51:674–680. https://doi.org/10.1016/j.optlaseng.2013.01.007

17. Demir AG, Colombo P, Previtali B (2017) From pulsed to continuous wave emission in SLM with contemporary fiber laser sources: effect of temporal and spatial pulse overlap in part quality. Int J Adv Manuf Technol. https://doi.org/10.1007/s00170-016-9948-7

18. Zhou X, Liu X, Zhang D et al (2015) Balling phenomena in selective laser melted tungsten. J Mater Process Technol. https://doi.org/10.1016/j.jmatprotec.2015.02.032

19. Suder WJ, Williams SW (2012) Investigation of the effects of basic laser material interaction parameters in laser welding. J Laser Appl 24:032009. https://doi.org/10.2351/1.4728136

20. Coroado J, Meco S, Williams S et al (2017). Fundamental understanding of the interaction of continuous wave laser with aluminium. https://doi.org/10.1007/s00170-017-0702-6

21. Banat D, Ganguly S, Meco S, Harrison P (2020) Application of high power pulsed nanosecond fibre lasers in processing ultra-thin aluminium foils. Opt Lasers Eng. https://doi.org/10.1016/j.optlaseng.2020.106075

22. Williams S, Suder W (2011) Use of fundamental laser material interaction parameters in laser welding. CLEO 2011 - Laser Sci to Photonic Appl 1–2

23. Suder W (2011) Study of fundamental parameters in hybrid laser welding. Dissertation, Cranfield University

24. Pan S, Yu G, Li S et al (2018) Application of millisecond pulsed laser for thermal fatigue property evaluation. Opt Laser Technol 99:382–391. https://doi.org/10.1016/j.optlastec.2017.09.026

25. Coroado J, Ganguly S, Suder W et al (2021) Selection of parameters in nanosecond pulsed wave laser micro-welding. Int J Adv Manuf Technol. https://doi.org/10.1007/s00170-021-07251-8

26. Ashby MF, Easterling KE (1984) The transformation hardening of steel surfaces by laser beams-I. Hypo-eutectoid steels Acta Metall. https://doi.org/10.1016/0001-6160(84)90175-5

27. TRUMPF (2014) 100W G4 pulsed fibre laser specification interface manual. TRUMPF Lasers UK Ltd, Southampton

28. Zang Z, Zeng X, Du J et al (2016) Femtosecond laser direct writing of microholes on roughened ZnO for output power enhancement of InGaN light-emitting diodes. Opt Lett 41:3463–3466. https://doi.org/10.1364/OL.41.003463

29. Quazi MM, Ishak M, Fazal MA et al (2020) Current research and development status of dissimilar materials laser welding of titanium and its alloys. Opt Laser Technol 126:106090. https://doi.org/10.1016/j.optlastec.2020.106090

30. Zwicker MFR, Moghadam M, Zhang W, Nielsen CV (2020) Automotive battery pack manufacturing – a review of battery to tab joining. J Adv Join Process 1:100017. https://doi.org/10.1016/j.jajp.2020.100017